Available online at www.sciencedirect.com
SCIENCE DIRECT®
Journal of Solid State Chemistry 177 (2004) 4672–4679
JOURNAL OF SOLID STATE CHEMISTRY
www.elsevier.com/locate/jssc

Stability of K_2CrO_4 to 50 GPa using Raman spectroscopy measurements

G. Serghiou*, C. Guillaume

School of Engineering and Electronics and Centre for Materials Science, University of Edinburgh, Kenneth Denbigh Building, Mayfield Road, Edinburgh, EH9 3JL, UK

Received 7 May 2004; received in revised form 7 July 2004; accepted 14 July 2004

Abstract

Raman spectroscopic measurements of K_2CrO_4 upon compression in an argon pressure medium reveal a series of structural transitions between ambient conditions and 50 GPa. The solid remains crystalline to the highest pressure measured. This behavior is consistent with an emerging trend upon compression for the extended class of A_2BX_4 solids which are isostructural to K_2CrO_4. In particular crystals with size ratios of anionic tetrahedral BX_4 groups to interstitial A cations below 1.45 remain crystalline at all pressures examined whereas those having ratios higher than 1.45 become amorphous.

Keywords: Pressure; Raman; Structural systematics; Stability; Molecular ionic solids

1. Introduction

Molecular ionic solids with the chemical formula A_2BX_4 (A = K, Rb, Cs; B = Cr, S, Cd, Se, Zn; X = O, Cl, Br, I) have been the focus of numerous studies revealing a multitude of phase transitions as a function of temperature and more recently pressure [1–3]. These phases include paraelectric, ferroelectric, ferroelastic as well as incommensurate modifications [3]. Despite the plethora of phases, the structures are all characterized by the same motif, namely isolated anionic tetrahedral BX_4 units with the interstitial sites being filled with A cations (Fig. 1) [3–8]. The most common modification prevalent at room temperature has orthorhombic symmetry with Pnma space group and four formula units per unit cell. The other modifications typically acquired at lower temperatures involve rotations of the tetrahedral units accompanied by readjustments in the interstitial cation positions [3,9,10]. These changes lead to doubling and tripling of the unit cell as the temperature is lowered, accompanied by concomitant increases in the number of formula units present in the unit cell. The most prevalent symmetry adopted at lower temperatures by these systems is monoclinic. These crystal–crystal transitions are in many instances bridged by incommensurate phases where the unit cell in the strict sense has an infinite size in one dimension. It has been found that the presence of large anionic BX_4 groups in relation to the size of the A cations, induces increased stresses in the backbone lattice resulting in an incommensurate modulation and strict loss of translational periodicity along a particular crystallographic axis [3–5,8]. In fact, the size threshold above which an incommensurate modulation arises for halides in this family is correlated with that found for crystalline to non-crystalline transitions upon compression, as documented by X-ray diffraction measurements [3,11]. This correlation was explained in terms of a packing of the anionic BX_4 units around the A cations. When the BX_4 units are small relative to the A cations (ex: $ZnCl_4$ to Cs^+), increased repulsive and steric stresses induced by pressure can be accommodated by deformations of the Cs^+ outer shell as opposed to significant changes in its

*Corresponding author. Fax: +44-131-650-6551.
E-mail address: george.serghiou@ed.ac.uk (G. Serghiou).

0022-4596/$ - see front matter © 2004 Elsevier Inc. All rights reserved.
doi:10.1016/j.jssc.2004.07.021

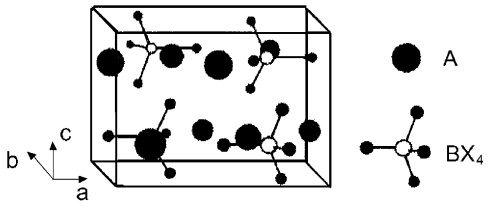

Fig. 1. Schematic of the experimentally determined average structure of A_2BX_4 molecular ionic solids ((A = K, Rb, Cs; B = Cr, S, Cd, Se, Zn; X = O, Cl, Br, I) in their orthorhombic Pnma phase which contains four formula units per unit cell. An essential way in which these systems differ from each other is via the ratios of the sizes of the anionic BX_4 tetrahedral units to that of the interstitial A cations ($(r_B + r_X)/r_A$, where r_i are the ionic radii) [4,5].

average position. In contrast to this, smaller A cations such as K^+ will accommodate increased stresses through larger and more varied displacements from their average positions resulting in a subsequent loss of translational periodicity at high pressures. The size ratio (s.r.), BX_4 to A, differentiating crystals that do lose translational periodicity from the rest was found to be about 1.45 [11].

This work expands investigation of the validity of the empirical size criterion governing the stability of A_2BX_4 molecular ionic solids at high densities. So far, our compressional study in this family using X-ray diffraction measurements to 60 GPa has included K_2ZnCl_4 (s.r. = 1.691), Rb_2ZnBr_4 (s.r. = 1.616), Rb_2ZnCl_4 (s.r. = 1.521), Cs_2ZnBr_4 (s.r. = 1.431), Cs_2ZnCl_4 (s.r. = 1.347), and K_2SeO_4 (s.r. = 1.225) [11]. We extend the compositional range and methodology here by examining the compressional behavior of orthorhombic K_2CrO_4 which has a BX_4/A ratio of 1.236 which falls below the BX_4/A size ratio threshold for transition to a non-crystalline state upon compression. We use Raman spectroscopy measurements, which are particularly sensitive to atomic rearrangements on the polyhedral level and complement previous X-ray diffraction measurements [12]. The only previous Raman spectroscopy measurements on K_2CrO_4 were to 4 GPa and no structural transitions were detected [13]. In early resistivity studies to 10 GPa on K_2CrO_4, Pistorius found evidence for three phase transitions at 2.6, 5.1 and 9.5 GPa at room temperature [14]. Pistorius and Rapoport though in a later study questioned these earlier results due to the presence of uniaxial stress, recrystallization, impurities as well as ambiguities in calibration procedures [15]. In this later study, using differential thermal analysis, Pistorius and Rapoport verified the well-known transition of ambient pressure orthorhombic K_2CrO_4 to a hexagonal modification above 942 K. Their data also suggested another phase transition of the ambient pressure orthorhombic phase above 2 GPa and 1323 K to a structure also suggested to have hexagonal symmetry. No phase transitions at ambient temperature were reported in this later study.

2. Experimental techniques

Single crystals of K_2CrO_4 (orthorhombic, space group Pnma, $Z = 4$, $a = 7.662$ Å, $b = 5.919$ Å, $c = 10.391$ Å, 99 + % purity Aldrich), were selected using a polarization microscope and Raman spectroscopy measurements [6,7,16]. Pressure was applied with a diamond anvil cell. The crystals, 10 μm thick and $50 \times 20\ \mu m^2$ horizontal dimensions, were placed in the centre of 301 stainless steel gaskets in an argon pressure medium. The sample chamber dimensions were between 130 and 150 μm in diameter and 60 μm in thickness. The Raman spectra were excited with the 457.9-nm line of an argon ion laser with powers ranging from 5 to 30 mW. The Raman spectra were analyzed in the 200–1150 cm^{-1} wavenumber range with a Spex 1402 double monochromator with a LN-cooled CCD (charged coupled device detector) with a spectral resolution of about 1 cm^{-1}. Pressure was measured using micron sized ruby chips placed next to the samples.

3. Results

Two experiments were performed, the first to 31 GPa, where the transformations were monitored upon compression and decompression, and the second to 51 GPa monitored upon compression. Because the single crystals placed in the cell in the two experiments did not have the same orientation, the ambient pressure spectra were not identical in each run. Factor group analysis for the Pnma symmetry allows in total, 18 internal modes ($6A_g + 3B_{1g} + 6B_{2g} + 3B_{3g}$) and 24 lattice modes, 18 of which are translational ($6A_g + 3B_{1g} + 6B_{2g} + 3B_{3g}$) and 6 of which are librational ($1A_g + 2B_{1g} + 1B_{2g} + 2B_{3g}$) [16]. At ambient pressure, the external and internal modes are situated in the 50–180 cm^{-1} and 300–950 cm^{-1} regions, respectively. In the first experiment 11 internal modes were detected and in the second experiment 10 internal modes were detected at ambient pressure, all belonging to stretching and bending modes of the CrO_4 tetrahedra (Table 1) [16]. No external modes were detected at ambient pressure because they lie at energies too low to detect by the experimental arrangement used, but several were detected above 10 GPa.

The effect of pressure on the Raman spectra of K_2CrO_4 in the two experiments are shown in Figs. 2 and 3. Figs. 2a and 2b show the effect of compression and decompression, respectively, on the Raman spectra in the first experiment. Figs. 3a and 3b show the effect of compression on the Raman spectra to 50.1 GPa in the

Table 1
Measured ambient pressure frequencies and vibrational assignments for K_2CrO_4 in the previous and the present study

K_2CrO_4, Pnma, $Z=4$ single crystal data (cm^{-1}) [16]	Vibrational assignment [16]	1st Expt (1 atm)	2nd Expt (1 atm)	Huang and Butler [13]
919	B_{2g}			919
905	A_g	906	906	907
	$(B_{1u}+B_{3u})$	890		
884	B_{2g}	886	886	
881	B_{1g}	883	883	880
877	B_{3g}	873	873	
868	A_g	866		869
852	A_g+B_{2g}	857	859	854
398	B_{2g}	398		397
397	A_g		395	
393	B_{3g}			
388	$B_{1g}+B_{2g}$	388	390	388
387	A_g		388	
352	B_{2g}	353	354	
351	B_{3g}	350	351	350
348	B_{1g}			
347	A_g			
182	B_{3g}			
181	A_{1g}			
164	$A_{1g}+B_{3g}$			
138	B_{1g}			
120	B_{2g}			
119	B_{3g}			
94	$B_{1g}+B_{3g}$			
87	B_{1g}			
84	A_{1g}			
58	B_{1g}			

Note: The first column shows the frequencies of all the modes observed in an ambient pressure orientation-dependent single crystal Raman spectroscopy study, in which all 18 internal, and 12 of the 24 lattice modes, were detected. The second column shows the vibrational frequency assignment based on the orientation-dependent single crystal measurements and the factor group analysis [16]. Columns three and four show the ambient pressure modes detected for experiments one and two, respectively, in the present study. In column three, the mode at 890 is likely due to an accidental IR active mode. Column five shows the ambient pressure modes detected in a previous compressional study to 4 GPa [13].

second experiment. The breaks in the spectra separate the low wavenumber (200–550 cm^{-1}) from the high wavenumber (800–1150 cm^{-1}) vibrational regions. The spectra within the two regions are scaled with respect to each other. Had all spectra been plotted on the same scale, the low wavenumber region spectra would be about an order of magnitude weaker in intensity than the high wavenumber region ones. In both Figs. 2 and 3, thick arrows designate the first pressure at which a new mode is detected above ambient pressure, and thin arrows designate the last pressure at which a mode is detected. The pressure dependence of the vibrational frequencies in the two experiments are shown in Figs. 4 and 5, respectively. The filled symbols designate compression and the open symbols decompression. Moreover, same symbols in the same wavenumber regime in the two experiments correspond to the same vibrational mode. The numerous changes in the Raman spectra occurring upon compression and decompression, are summarized below. The lattice mode changes are described last for each run since they are not detectable below 10 GPa.

In the first experiment, the following changes were documented upon compression (Figs. 2a and 4) and decompression (Figs. 2b and 4). At between 0 and 6.5 GPa one new mode appears, situated at 407 cm^{-1} at 6.5 GPa. This mode persists to 31 GPa upon compression and can be monitored to 1.1 GPa upon decompression. Additionally, at between 0 and 6.5 GPa two modes situated at 883 and 890 cm^{-1} at ambient pressure, vanish. Upon decompression the 890 cm^{-1} mode reappears below 8.2 GPa, situated at 914 cm^{-1} at 4.4 GPa and the 883 cm^{-1} mode reappears below 4.4 GPa, situated at 905 cm^{-1} at 3.3 GPa. A further new mode appears as a shoulder at 10.9 GPa, remains a weak shoulder until 18.8 GPa and emerges as a distinct peak at 21.2 GPa situated at 411 cm^{-1}. This mode is clearly visible up to 23.8 GPa. Upon decompression it becomes visible between 27.8 and 24.7 GPa, is situated at 416 cm^{-1} at 22.4 GPa, becomes a shoulder below

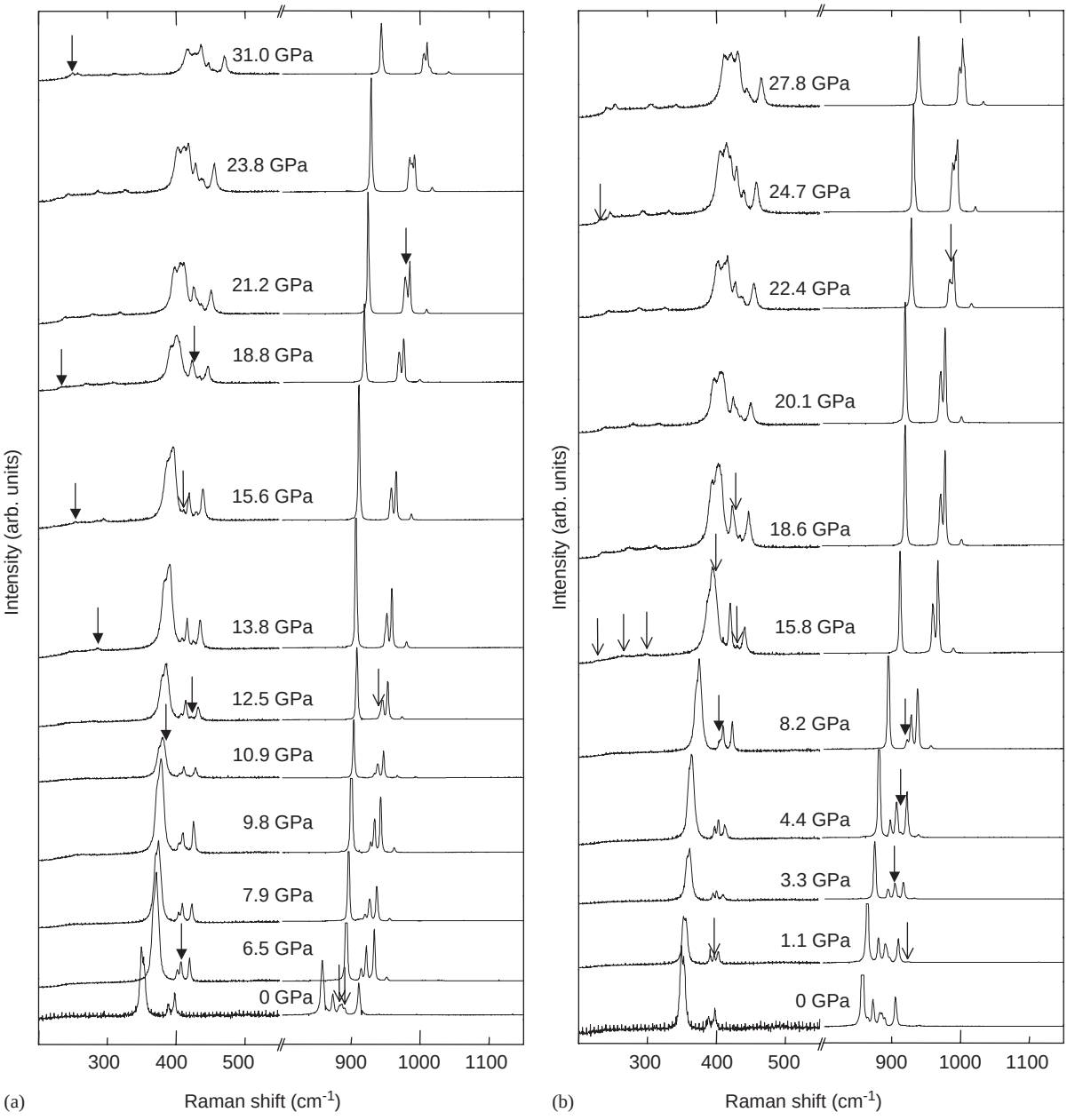

Fig. 2. Effect of pressure on the Raman spectrum of K_2CrO_4 upon compression and decompression to 31 GPa in the first experiment. (a) and (b) show the effect of pressure on the spectra upon compression and decompression, respectively.

20.1 GPa and disappears below 15.8 GPa. At 12.5 GPa another new mode emerges, situated at 425 cm^{-1} at 13.8 GPa. This mode persists to 31 GPa and disappears upon decompression at between 15.8 and 8.2 GPa. Moreover, at between 12.5 and 13.8 GPa a mode situated at 873 cm^{-1} at room pressure vanishes, and reappears at between 15.8 and 8.2 GPa upon decompression. Above 15.6 GPa, a further new mode appears situated at 431 cm^{-1} at 21.2 GPa which persists to 31 GPa and vanishes at between 18.6 and 15.8 GPa upon decompression. Also at between 15.6 and 18.8 GPa another mode, located at 389 cm^{-1} at ambient pressure and at 411 cm^{-1} at 15.6 GPa, vanishes, and reappears at between 15.8 and 8.2 GPa upon decompression. Finally, at 18.8 GPa the intense highermost energy doublet becomes less well resolved than at 15.6 or 13.8 GPa and at 21.2 GPa the lower energy mode of the doublet becomes more clearly asymmetric. At 23.8 GPa, a distinct peak emerges at 988 cm^{-1} between the doublet. This new peak becomes even stronger at 31.0 GPa and disappears upon decompression at between 22.4 and 18.6 GPa. The following changes were documented for the lattice modes upon compression and decompression. At 13.8, 15.6 and 18.8 GPa three modes becomes

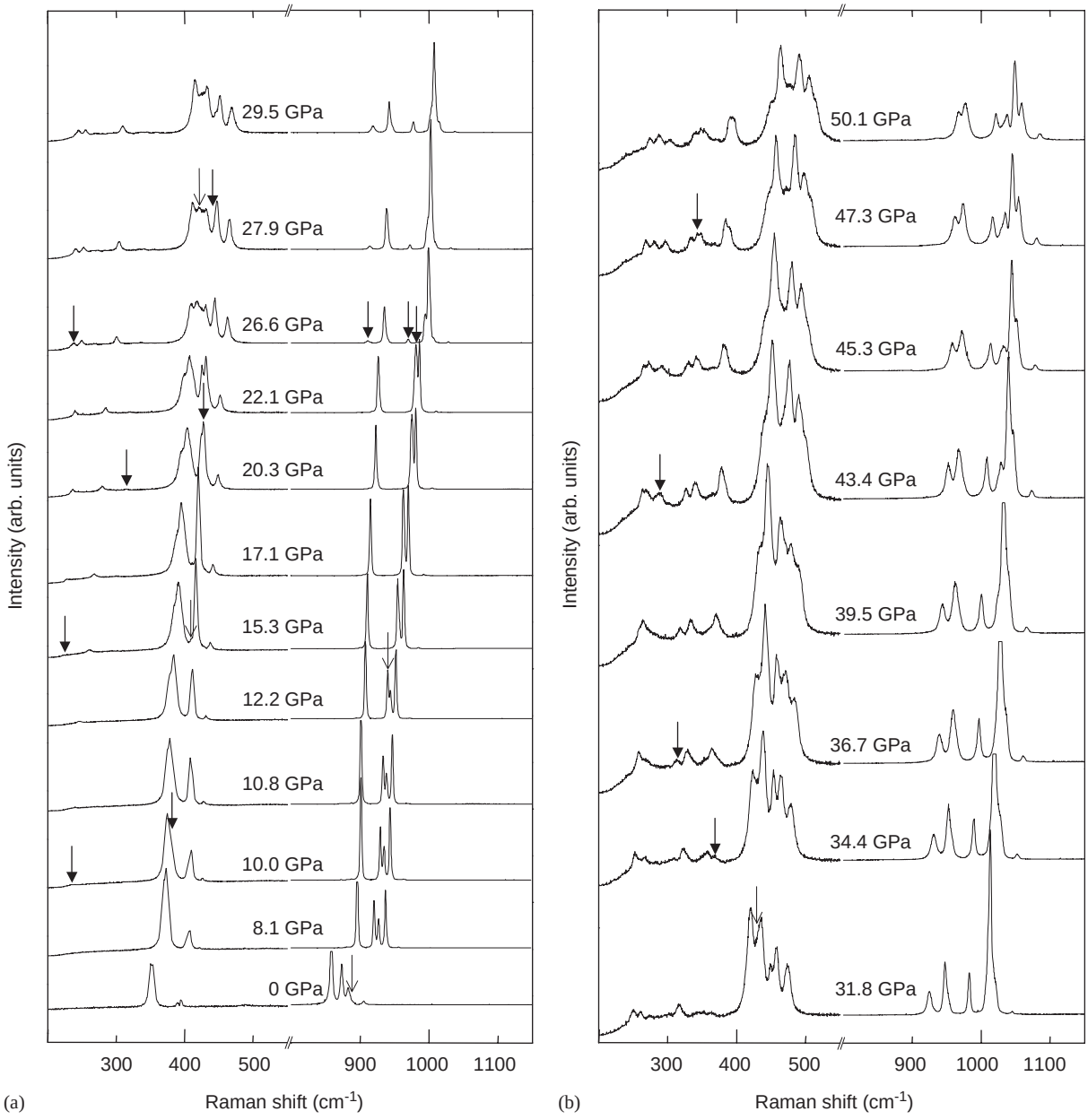

Fig. 3. Effect of pressure on the Raman spectrum of K_2CrO_4 upon compression to 50.1 GPa in the second experiment. (a) and (b) show the effect of pressure on the spectra upon compression in the ambient to 29.5 and 31.8 to 50.1 GPa regimes, respectively.

detectable at 286, 253 and 234 cm^{-1}, respectively. These modes persist to 31 GPa and vanish below 15.8 GPa upon decompression. A further mode was detected at 31 GPa at 249 cm^{-1}, which vanished upon decompression between 24.7 and 22.4 GPa.

In the second experiment to 50.1 GPa the following changes in the spectra were documented (Figs. 3 and 5). At between 0 and 8.1 GPa an ambient pressure vibrational mode located initially at 886 cm^{-1} vanishes. At between 8.1 and 10 GPa a new mode appears, situated at 380 cm^{-1} at 10.0 GPa. This mode vanishes at between 31.8 and 34.4 GPa. Between 12.2 and 15.3 GPa, a second mode located at ambient pressure at 873 cm^{-1} and at 12.2 GPa at 941 cm^{-1} vanishes. At between 15.3 and 17.1 GPa, a mode present at ambient pressure as a weak shoulder at 388 cm^{-1} also disappears. At between 17.1 and 20.3 GPa a new mode appears, situated at 428 cm^{-1} at 20.3 GPa. This mode shifts to higher wavenumbers and persists to the highest pressures measured of 50.1 GPa. At 20.3 GPa the intense higher-most energy doublet becomes less well resolved than at 17.1 or 15.3 GPa and at 22.1 GPa the lower energy mode of the doublet becomes more clearly asymmetric. At the next measured pressure of 26.6 GPa, a distinct strong

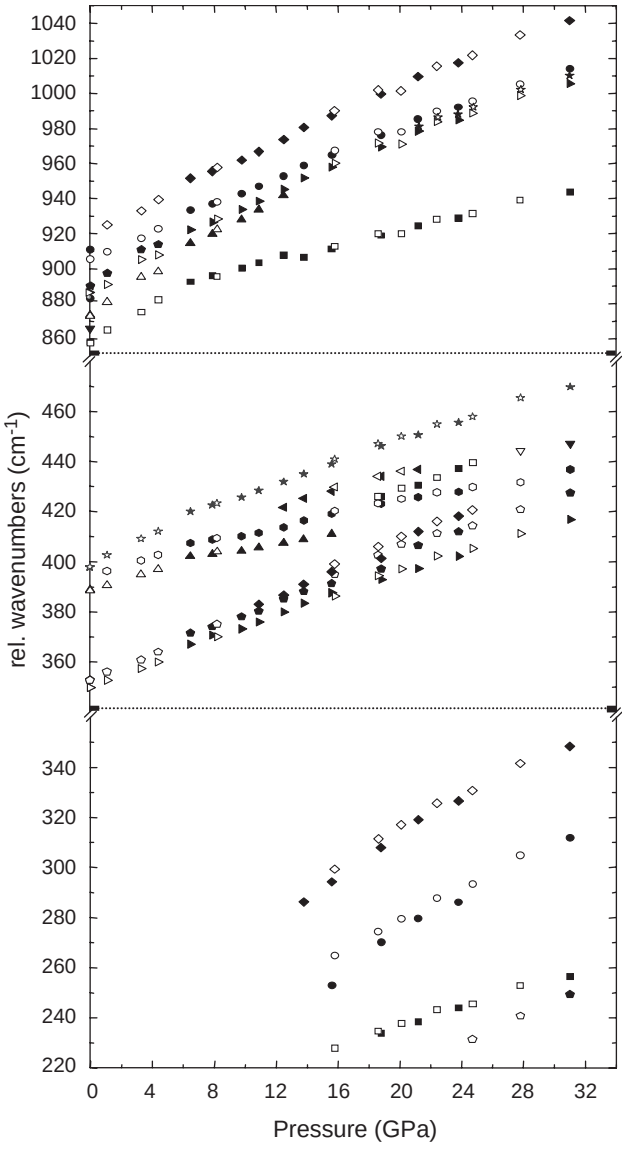

Fig. 4. Pressure dependence of the Raman frequencies upon compression and decompression to 31.0 GPa in the first experiment. The lattice modes shown in the 220–350 cm^{-1} region could only be measured above about 10 GPa.

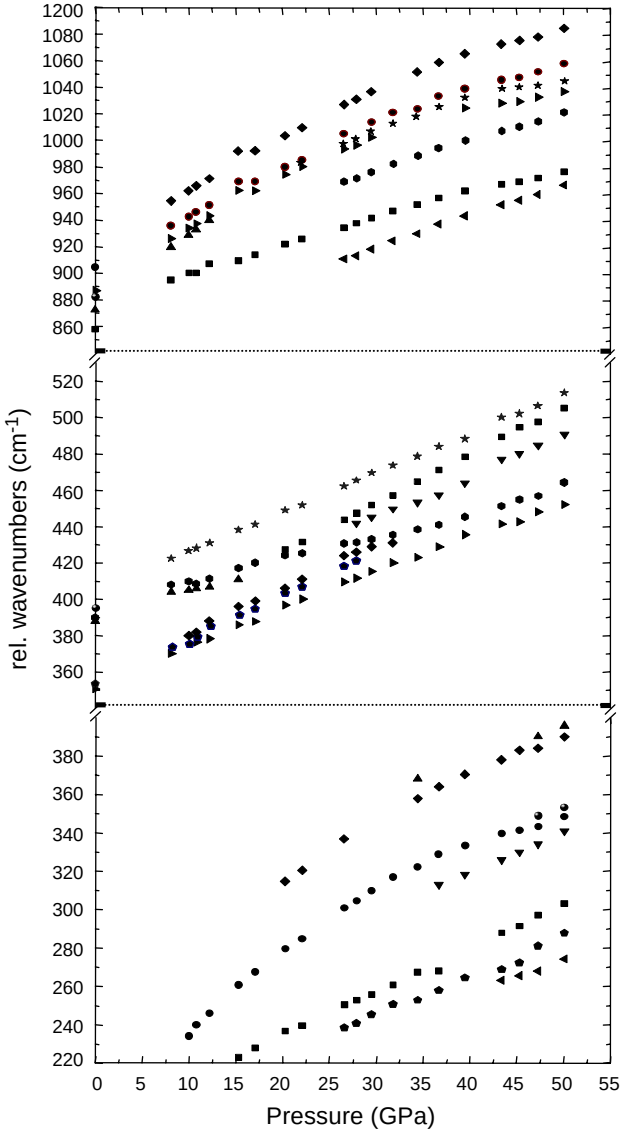

Fig. 5. Pressure dependence of the Raman frequencies upon compression to 50.1 GPa in the second experiment. The lattice modes shown in the 220–400 cm^{-1} region could only be measured above about 10 GPa.

peak emerges at 1000 cm^{-1} between the doublet which also persists to 50.1 GPa. At between 22.1 and 26.6 GPa, two further new modes emerge located at 912 and 970 cm^{-1} at 26.6 GPa, both of which also persist to 50.1 GPa. Additionally a new mode emerges at between 27.9 and 29.5 GPa, situated at 450 cm^{-1} at 31.8 GPa which also persists to 50.1 GPa. Moreover, a mode located at 354 cm^{-1} at ambient pressure, vanishes at between 27.9 and 29.5 GPa. The following changes were documented for the lattice modes. A lattice mode becomes detectable at 10 GPa at 233 cm^{-1} and persists to 50.1 GPa. A further mode appears at 223 cm^{-1} at 15.3 GPa which persists to 50.1 GPa as well. Additionally two further modes appear at 315 cm^{-1} at 20.3 GPa and 239 cm^{-1} at 26.6 GPa, which also persist to 50.1 GPa. Finally, four further weak lattice modes emerge at 368 cm^{-1} at 34.4 GPa, at 313 cm^{-1} at 36.7 GPa, at 269 cm^{-1} at 43.4 GPa, and at 349 cm^{-1} at 47.3 GPa. All of these also persist to the highest pressures measured of 50.1 GPa.

4. Discussion

The most general result is that the new data support our earlier findings that the BX_4/A size ratio serves as an effective and simple empirical criterion for predicting the stability of A_2BX_4 (A = K, Rb, Cs; B = Cr, S, Cd, Se, Zn; X = O, Cl, Br, I) molecular ionic solids based on the

Pnma space group upon compression [11]. The trend namely is that solids in this family with size ratios greater than 1.45 lose translational periodicity, whereas those with size ratios below this value retain their crystallinity. With respect to the more detailed structural rearrangements taking place upon compression we first note that the compressional behavior of solids within this family at pressures high enough to investigate their stability with respect to loss of translational periodicity had only been investigated using X-ray diffraction [11,12]. Raman spectroscopic measurements within this class had been limited to pressures below about 20 GPa so far [17–19]. In particular, Raman spectroscopy measurements on K_2CrO_4 had only been performed to 4 GPa revealing no structural changes [13]. Angle dispersive X-ray diffraction measurements also revealed no phase transitions to 50 GPa and hence that the ambient pressure orthorhombic (Pnma) crystal structure was retained at all pressures [12]. A decrease in the relative intensity of diffraction peaks associated with the CrO_4 tetrahedra was attributed to static orientational disorder in the oxygen sublattice. Our high-pressure Raman spectra reveal, as described above, a series of structural changes as evident from the appearance of several new vibrational modes and the disappearance of others between ambient pressure and 50.1 GPa, but show no evidence for peak broadening and overall decline in intensity. There are however previous studies on A_2BX_4 molecular ionic solids indicating that the number of Raman active modes observed in A_2BX_4 solids may be more or even less than those allowed by the crystal symmetry [8,20–25]. For example in K_2SeO_4, the observation of a larger number of internal modes than that predicted by its X-ray- determined Pnam structure was explained in terms of selenate tetrahedra (SeO_4) that are perturbed slightly off their ideal positions dictated by the orthorhombic structure with Pnam space group. This resulted in the lifting of degeneracies by the influence of the cation sublattice crystal field [21,23,26]. In Rb_2ZnCl_4, both lifting of degeneracies similar to K_2SeO_4, as well as reduction in the number of certain vibrational modes with respect to those predicted by the orthorhombic Pnam phase have been observed in the internal mode region. The explanation for the former is similar to that for K_2SeO_4. The explanation for the reduced splittings, based on molecular dynamic simulations, was in terms of rotations of the $ZnCl_4$ anions away from their exact crystallographical positions, into more energetically favorable configurations where their local internal stresses and the associated splittings of the free ion degeneracies are least [8–9,22]. Raman scattering being a local to medium range order probe is more sensitive to these local rearrangements whereas X-ray diffraction may only give the experimentally determined time averaged structure [8,23].

Nevertheless the higher pressure spectra differ notably from the ambient pressure one, pointing at phase transitions. It is also the case that more than 25 different structures with different space groups can be attained by suitable small reorientations of the prototype orthorhombic structure which can have between 4 and 28 formula units per unit cell or even, an infinite number for the case of incommensurate phases [3,10,27]. Thus an unambiguous detailed correlation of the high-pressure spectral changes with a unique structure is difficult even if K_2CrO_4 at 50.1 GPa still consists of isolated tetrahedral (CrO_4) [16,28] albeit densely packed around the potassium counteractions.

5. Conclusions

It would be important to compare the high-pressure Raman spectra of systems that do not lose translational periodicity at high densities such as K_2CrO_4 with those that do in order to evaluate the contrasting behavior on the polyhedral level. In particular, there has been recent work suggesting that loss of order upon compression in many systems takes place in two steps [29,30]. The first step involves anionic sublattice disorder and the second, complete loss of translational periodicity. The anionic sublattice in the A_2BX_4 system, would be comprised of the X anions. For example in Rb_2ZnCl_4, as the large $ZnCl_4$ units pack around the rubidium cations they distort, leading to an increasingly varied array of Zn–Cl vibrations (and hence Cl^- positions) which would ultimately cause broadening and precipitous decline in intensity of the internal vibrational modes. This would then be followed by progressively more pronounced perturbations of the underlying cationic backbone lattice leading to the observed loss of translational periodicity at a pressure of about 40 GPa [11].

In fact the backbone lattice concept is consistent with the compressional behavior of systems which can be viewed as not having a backbone lattice at all, namely BX_4 crystals (B = Sn, Ge and X = I, Br, Cl), which consist solely of isolated tetrahedral units with no A counteractions in the interstitial sites [31,32]. All of these amorphize at pressures above 8–10 GPa [33–36]. One can venture to the other structural limit as well where there are no BX_4 units but only A counteractions, transforming the A_2BX_4 solids into alkali metals. These can then be viewed as systems which consist solely of a backbone lattice that would not lose translational periodicity at any pressure. The compressional behavior of alkali metals is certainly consistent with this behavior since they remain crystalline at all pressures measured spanning the range from ambient to 200 GPa [37,38]. Thus considering the cationic sublattice as the controlling factor in the stability of these crystals, then, when there are no A cations, the crystal will easily lose

translational periodicity. When A counteractions are introduced, and as the BX_4 over A size ratio becomes smaller, the crystals become increasingly resistant to disordering. There have, in fact, been numerous recent studies indicating that the stability of crystals including ones examined here, is primarily determined by the highly symmetrical potential of the cations, and that the anions act simply as a pressure perturbation on the backbone cationic lattice [39–41]. Clearly, considerable high-resolution diffraction and light-scattering studies are still required, to test and refine these findings so that we can ultimately develop predictive ability on the role of polyhedral units and cationic and anionic sub-networks in governing the stability of solids.

Acknowledgments

We thank Reinhard Boehler and the Max Planck Institute for Chemistry for support and provision of facilities.

References

[1] A. El-Korashy, K.J. Roberts, J. Phys. Chem. Solids 64 (2003) 2133.
[2] T. Asahi, K. Hasebe, J. Phys. Soc. Japan 71 (2002) 2925.
[3] H.Z. Cummins, Phys. Rep. 185 (1990) 211.
[4] I. Etxebarria, J.M. Perez-Mato, G. Madariaga, Phys. Rev. B 42 (1990) 8482.
[5] I. Etxebarria, J.M. Perez-Mato, G. Madariaga, Phys. Rev. B 46 (1992) 2764.
[6] W.H. Zachariasen, G.E. Zeigler, Z. Kristallogr 80 (1931) 164.
[7] K. Toriumi, Y. Saito, Acta Crystallogr B 34 (1978) 3149.
[8] V. Katkanant, J.R. Hardy, R.D. Kirby, F.G. Ullman, Ferroelectrics 99 (1989) 213.
[9] H.M. Lu, J.R. Hardy, Phys. Rev B 45 (1992) 7609.
[10] M. Kurzynski, Acta Phys. Pol. B 26 (1995) 1101.
[11] G. Serghiou, H.-J. Reichmann, R. Boehler, Phys. Rev. B 55 (1997) 14765.
[12] C.M. Edwards, J. Haines, I.S. Butler, J.-M. Leger, J. Phys. Chem. Solids 60 (1999) 529.
[13] Y. Huang, I.S. Butler, Appl. Spectrosc 44 (1990) 1326.
[14] C.W.F.T. Pistorius, Z. Phys. Chem. Neue Folge 35 (1962) 109.
[15] C.W.F.T. Pistorius, E. Rapoport, J. Phys. Chem. Solids 30 (1969) 195.
[16] D.M. Adams, M.A. Hooper, M.H. Lloyd, J. Chem. Soc. A (1971) 946.
[17] K.M. Yenice, S.A. Lee, J. Raman Spectrosc 23 (1992) 299.
[18] T.R. Ravindran, A.K. Arora, High Pressure Res 16 (1999) 233.
[19] T. Sakuntala, A.K. Arora, Advances in High Pressure Science and Technology, University Press, Hyderabad, 1997, p.76.
[20] A.N. Vtyurin, A.G. Ageev, A.S. Krylov, I.V. Shmygol, Ferroelectrics 56 (1999) 51.
[21] P. Echegut, F. Gervais, N.E. Massa, Phys. Rev. B 34 (1986) 278.
[22] V. Katkanant, F.G. Ullman, P.J. Edwardson, J.R. Hardy, Technical Report, Defense Technical Information Centre (DTIC), Report No. NTIS AD-A172 71, 1986.
[23] N.E. Massa, F.G. Ullman, J.R. Hardy, Phys. Rev. B 27 (1983) 1523.
[24] I. Noiret, Y. Guinet, A. Hedoux, Phys. Rev. B 52 (1995) 13206.
[25] R. Frech, G. Dharmasena, J.Chem. Phys 102 (1995) 6941.
[26] P. Echegut, F. Gervais, N.E. Massa, Phys. Rev. B 31 (1985) 581.
[27] M. Kurzynski, Phase Transit 52 (1994) 1.
[28] S. Montero, R. Schmolz, S. Haussuhl, J. Raman Spectrosc 2 (1974) 101.
[29] J.H. Nguyen, M.B. Kruger, R. Jeanloz, Phys. Rev. Lett 78 (1997) 1936.
[30] A.K. Arora, R. Nithya, T. Yagi, N. Miyajima, T.A. Mary, Solid State Commun 129 (2003) 9.
[31] Y. Fujii, M. Kowaka, A. Onodera, J. Phys. C 18 (1985) 789.
[32] S.M. Sharma, S.K. Sikka, Progr. Mater. Sci 40 (1996) 1.
[33] S. Sugai, J. Phys. C 18 (1985) 799.
[34] A.L. Chen, P.Y. Yu, Phys. Rev. B 44 (1991) 2883.
[35] W. Williamson, S.A. Lee, Phys. Rev. B 44 (1991) 9853.
[36] G.R. Hearne, M.P. Pasternak, D.R. Taylor, Phys. Rev. B 52 (1995) 9209.
[37] W.B. Holzapfel, Rep. Progr. Phys 59 (1996) 29.
[38] M.I. Katsnelson, G.V. Sinko, N.A. Smirnov, A.V. Trefilov, K.Y. Khromov, Phys. Rev. B 61 (2000) 14420.
[39] A. Vegas, A. Grzechnik, K. Syassen, I. Loa, M. Hanfland, M. Jansen, Acta Crystallogr B 57 (2001) 151.
[40] A. Vegas, A. Grzechnik, M. Hanfland, C. Muhle, M. Jansen, Solid State Sci 4 (2002) 1077.
[41] A. Vegas, M. Jansen, Acta Crystallogr. B 58 (2002) 38.